Journal of Advanced Research in Fluid Mechanics and Thermal Sciences

Journal homepage:
https://semarakilmu.com.my/journals/index.php/fluid_mechanics_thermal_sciences/index
ISSN: 2289-7879

Synthesis and Characterization of Activated Carbon Derived from Rubberwood Sawdust via Carbonization and Chemical Activation as Electrode Material for Supercapacitor

Supawet Phainuphong[1], Juntakan Taweekun[2,*], Kittinan Maliwan[2], Thanansak Theppaya[2], Md Sumon Reza[2,3], Abul Kalam Azad[3]

[1] Energy Technology Program, Faculty of Engineering, Prince of Songkla University, Hatyai, Songkhla 90112, Thailand
[2] Department of Mechanical and Mechatronics Engineering, Faculty of Engineering, Prince of Songkla University, Hatyai, Songkhla, 90112, Thailand
[3] Faculty of Integrated Technologies, Universiti Brunei Darussalam, Jalan Tungku Link, Gadong BE, 1410, Brunei Darussalam

ARTICLE INFO

Article history:
Received 13 January 2022
Received in revised form 28 March 2022
Accepted 30 March 2022
Available online 19 April 2022

Keywords:
Activated carbon; chemical activation; electrode material; rubberwood sawdust; supercapacitor

ABSTRACT

This research aims to study the physical and electrochemical properties of the activated carbon derived from rubberwood sawdust as electrode material for supercapacitors. Rubberwood sawdust, waste from the wood processing industry, was used as the precursor for synthesizing activated carbon using potassium hydroxide (KOH) as an activation agent. The carbonization was carried out at 400 °C under the nitrogen atmosphere. In this experiment, the rubberwood sawdust chars were activated by impregnating KOH solution using the impregnation ratios 1:1 and 1:3 (Char: KOH). After that, the samples were activated at 700 °C, 800 °C and 900 °C, respectively. The adsorption isotherm, surface area, total pore volume, pore size distribution, and structure porosity were investigated. The XRD was used to examine the structural characteristics. The morphology of the sample was characterized by FESEM. The surface functional group of the samples was determined by FTIR and Raman spectroscopy. The three-electrode testing consists of the activated carbon samples coated on aluminum foil (Working electrode), Ag/AgCl (Reference electrode), and platinum wire (counter electrode) in 1 molar of KOH. According to the research, the activated carbon at an impregnation ratio of 1:3 with an activation temperature of 900 °C presented the highest surface area, total pore volume, and average pore diameter as 1,574.39 m^2/g, 0.6906 cm^3/g, and 1.89 nm, respectively. The cyclic voltammetry (CV) result showed a high specific capacitance value of 54.08 F/g at a scan rate of 5 mV/s in the case of the impregnation ratio of 1:3 with an activation temperature of 900 °C. Thus, the activated carbon derived from rubberwood sawdust waste as an electrode material can be a promising candidate for supercapacitors due to its outstanding electrochemical properties.

* *Corresponding author.*
E-mail address: juntakan.t@psu.ac.th

https://doi.org/10.37934/arfmts.94.2.6176

1. Introduction

The rapid development of the community and the continuous evolution of technologies lead to high energy demand, which results in shortages of fossil fuels and increased environmental contamination. The utilization of renewable energy is an exceptionally essential key to solving these problems [1,2]. The energy storage device is also required because it is the primary equipment to handle the unstable electricity generated from renewable energy. Supercapacitors are electrochemical capacitors with a greater energy density than capacitors and a higher power density than batteries [3]. They can be applied in many electronic devices and energy storage because of their quick charge/discharge rate, long cycle life, and eco-friendly [4,5].

Supercapacitors are classified into two mechanisms of charging storage. The first type is electrical double-layer capacitance (EDLC). The energy is stored via electrostatic reversibility of ions between electrode-electrolyte with double layer formation [6]. Porous carbon materials are generally used as electrode materials in this type. The second type is pseudo capacitance, related to surface redox reactions. Generally, conducting polymers, metal, and metal oxide are used as electrode materials in the second type [7]. The electrode material plays a significant role in improving the performance of supercapacitors. Carbon-based materials, such as carbon nanotubes, graphite, and graphene, with a high specific surface area, good conductivity, chemical stability, and long life cycle, are suitable for electrode material [8]. However, the mass production of these carbon materials is complex synthetic and high-cost raw materials. The activated carbon derived from biomass is a good choice for the low cost-effective precursors and easy to prepare porous carbon materials due to their abundance, high carbon composition, and cheapness [9,10]. Many biomass materials such as oil palm empty fruit bunches, cassava peel waste, chestnut wood, cotton stalk, waste coffee beans, waste tea leaves, sunflower seed shell, argan seed shells, banana peel, cucumis melo peel, polyalthia longifolia seeds, coconut shell, bamboo and rubberwood seed shell are used as electrode materials in last decade [11-25]. Since the rubber tree is abundantly planted in the south of Thailand, Rubberwood is mostly utilized as a raw material in the furniture industry. After production, raw material residue generates waste like slabs and sawdust. Thus, in this research, the rubberwood sawdust was used as precursor material to add their values.

Generally, the activated carbon can be prepared by two methods. The first method is physical activation. CO_2 or steam is used to activate the raw ingredients at high temperatures ranging from 700 °C to 1100 °C. However, the activated carbon derived from this method has a low surface area [26]. The second method is chemical activation, which involves using a chemical agent to impregnate carbon-based materials and activate at a temperature range of 300 °C to 800 °C under an inert atmosphere. During the chemical activation process, Chemical agents are employed to dehydrate the raw material and remove the tar or volatile matter. It also enhances the surface area and porosity [27]. Generally, the chemical activation agents, such as the acidic group; H_2SO_4, H_3PO_4, the alkaline group; KOH, NaOH, and the metallic salt; $ZnCl_2$, are used as a chemical activation agent [28]. Since the KOH is less corrosive and environmentally friendly, it is a good alternative for chemical activation [29]. It also produces micropores and mesopores, suitable for various applications [30]. In addition, the Impregnation ratio is a significant parameter for chemical activation to achieve a high surface area and superior pore volume [31].

Usually, the double-layer capacitors (DLC) represent the higher energy density and higher capacity per volume among capacitors [32]. Also, electrolytes play an essential role in electrical double layer capacitance performance. Many researchers reported that electrodes from activated carbon exhibit good electrochemical properties in KOH electrolytes [33]. Elaiyappillai *et al.,* [20]

studied the three electrodes system in 1 M of KOH due to a high specific capacitance of 376 F/g. Thus, the KOH aqueous electrolytes have an excellent choice for the working electrodes due to their environmentally friendly, inexpensive, and uncomplicated preparation [20].

In this study, the synthesis of high porous carbons derived from rubberwood (Hevea brasiliensis) sawdust is determined by the simple carbonization and chemical activation with KOH as an activation agent at the impregnation ratios of 1:1 and 1:3 with the activation temperature of 700-900 °C. The samples were characterized to analyze their structure, textural characterization, surface morphology, and capacitive properties of EDLC by using three-electrode testing in KOH as electrolyte. To the best of our knowledge, very few studies have been carried out to prepare activated carbon from the rubberwood sawdust available in Thailand by the chemical (KOH) activation as aforementioned for supercapacitor applications.

2. Methodology

2.1 Materials

The dried rubberwood sawdust was collected from Southern Biomass Fuel Co., Ltd, Songkhla province, Thailand. Potassium hydroxide pellets (KOH) and hydrochloric acid (37 wt%, HCl) were bought from Molecule Co., Ltd (Thailand). Chemical agents Nmethyl-2-pyrrolidone (NMP), polyvinylidene fluoride (PVDF), and conductive carbon black were purchased from Dongguan Gelon LIB Co., Ltd (China). Aluminum foil (16μm thickness) was obtained from Xiamen Tob New Energy Technology Co., Ltd (China).

2.2 Preparation of Activated Carbon Derived Rubberwood Sawdust (RS)

In two stages, the activated carbon (AC) was prepared from rubberwood sawdust as the staple. The first step was the carbonization process, and the second step was the chemical activation process. In the first step, the rubberwood sawdust (RS) was cleaned up with purified water to eliminate impurities and dust; then, it was dried in an oven at 110 °C overnight to diminish moisture content. Further, the sample was placed in the circular tube furnace, heated up to 400 °C at a heating rate of 6 °C/min, maintained for 1 hour under a nitrogen gas atmosphere, and cooled to room temperature. The obtained carbonized rubberwood sawdust char was labeled as RS-Char.

In the second step, chemical activation was carried out using 50 g of RS-Char and 50-150 g of potassium hydroxide (KOH) to produce the impregnation ratios of 1:1 and 1:3. The chemical activating agent was dissolved in 300 ml of purified water to provide the KOH solution. The RS-Char and KOH solution was stirred using a magnetic stirrer for 24 hours. After that, the well-mixed slurry was heated at 700-900 °C (heating rate of 6 °C/min) for 3 hours under a nitrogen gas atmosphere. After cooling to room temperature, the AC was submerged in 0.1 molars of hydrochloric acid (HCl) for 3 hours at environment temperature before being cleaned with deionized water to achieve a neutral pH. The AC samples were dried in an oven at 110 °C for 12 hours and maintained in a desiccator silica gel to avoid moisture. The AC samples were tagged as RS1:1-800, RS1:3-700, RS1:3-800, and RS1:3-900, respectively. Figure 1 shows the schematic preparation of activated carbon samples.

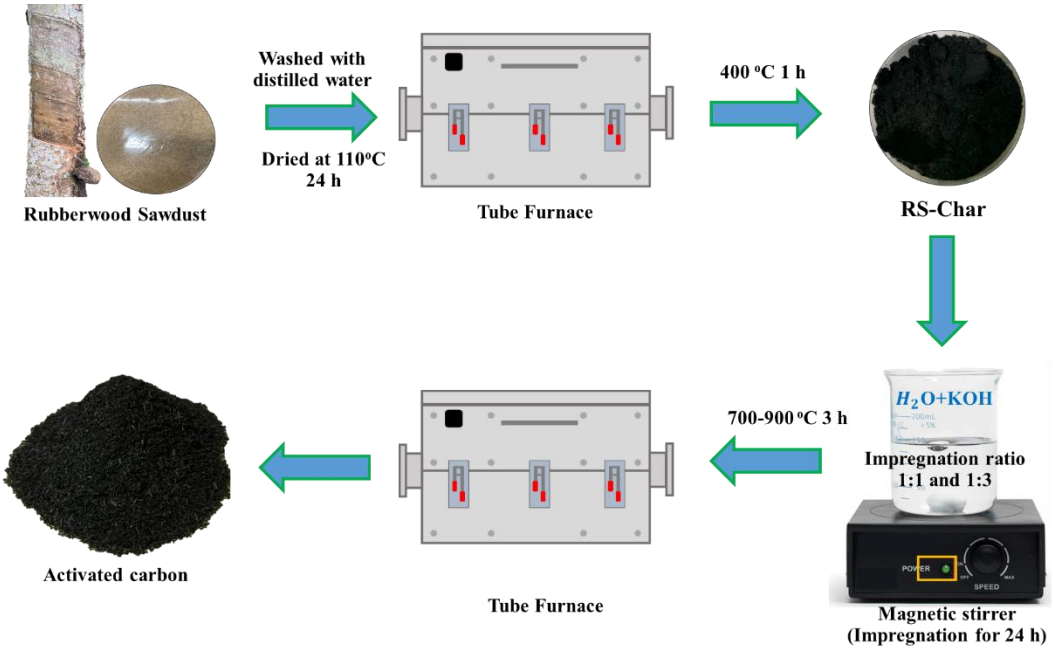

Fig. 1. The schematic preparation of activated carbon samples

2.3 Characterization of Rubberwood Sawdust Char and Activated Carbon

The four digits scale was used to weigh the samples and the precursor materials. The fixed carbon, moisture, ash, and volatile matter were evaluated by TGA 701, LECO, USA (based on ASTM D7582-15). The CHNS/O analyzer detected the elemental components of rubberwood sawdust, char, and AC by using the dynamic flash combustion technique (WI-RES-CHNS/O-002), Flash 2000, Thermo scientific, Italy. The Brunauer-Emmett-Teller (BET) surface area analysis of the RS samples was analyzed using Micromeritics ASAP2460 high throughput surface area and porosity analyzer. In addition, FT-IR spectra of the RS samples were analyzed by Bruker/ VERTEX70 spectrometer. X-ray diffraction (XRD) of the AC samples was recorded using an Empyrean/ PANalytical Empyrean diffractometer. Raman spectra were carried out using RAMANtouch (force)/ Nanoproton RAMANtouch (force), Raman spectrometer from the office of Scientific Instrument and Testing at Prince of Songkhla University, Thailand. Field Emission Scanning Electron Microscope (FESEM) images from the Center for Scientific and Technological Equipment, Walailak University, Thailand. The Merlin compact, ZEISS Microscopy detected the Energy Dispersive X-ray (EDX) spectroscopy of the RS samples.

2.4 Electrochemical Measurements

The electrochemical measurements of RS activated carbons were performed by Metrohm, Autolab/ PGSTAT 302N potentiostat analyzer at Metallurgy and Materials Science Research Institute, Chulalongkorn University, Thailand. The three-electrode system was applied in 1 M KOH at room temperature with a Platinum wire as a counter electrode, Ag/AgCl as a reference electrode, and RS samples coated on aluminum foil as a working electrode. The working electrode was prepared by mixing electrode material (RS-derived activated carbon), polyvinylidene fluoride (PVDF), and conductive carbon black with the ratio of 8:1:1 through N-methyl pyrrolidone (NMP) solvent. The slurry of electrode material was coated on aluminum foil by using a doctor blade with a wet film thickness of 250 µm. After that, it was dried at 80 °C in an oven for 6 hours to remove the NMP solvent. The average mass loading of the working electrode was approximately around 2 mg (1 cm ×

1 cm). The cyclic voltammetry (CV) was performed at different scan rates between 5-100 mV/s. The specific capacitance (C_{sp}) values for the three-electrode systems of RS activated carbon samples were calculated from CV measurement using Eq. (1) [20,21]. The electrochemical impedance spectroscopy (EIS) was carried out in the frequency range between 100 kHz to 0.1 Hz with an amplitude of 10 mV.

$$C_{SP} = \int \frac{\Delta I}{2Vm\left(V_2 - V_1\right)} \; \therefore \Delta I = I_a - I_c \tag{1}$$

Where, C_{sp} (F/g) denotes the specific capacitance of the three-electrode system, ΔI/2 presents the half of the integration area of the CV curve, I_a and I_c are the anodic and cathodic current, V refers to the scan rate, m (g) represents the mass of the electrode material, and V_2-V_1 is the potential difference on the CV curve.

3. Results

3.1 Proximate and Ultimate Analysis

The proximate and ultimate analyses of the RS samples are shown in Table 1. The volatile matter, fixed carbon, moisture, and ash were acquired using the thermogravimetric diagnosis. The rubberwood sawdust (RS) is raw material containing high volatile matters, fixed carbon, moisture, and ash of 74.05, 15.76, 7.71, and 2.48% by weight. These values are comparable with the results of other biomasses [34,35]. After carbonization into RS-Char, it indicated lower volatile matters, a remarkable increase of fixed carbon, less moisture, and ash of 31.84, 60.09, 4.04, and 4.03%, respectively. The higher amount of fixed carbon was due to the elimination of volatile matter at higher temperatures in the pyrolysis process [36]. The results also revealed that RS1:3-800 had the lowest value of volatile matters, the highest value of fixed carbon, and the lowest value of moisture and ash, equal to 12.53, 80.37, 3.28, 3.82%, respectively. For the ultimate analysis, the number of elements was performed by the CHNS/O analyzer. The RS contained C, H, O, N, S of 45.06, 6.05, 45.28, 0.15, 0.07%, respectively. These values also correspond to the results of biomasses such as pine sawdust and paulownia wood [37,38]. After carbonization, the RS-Char exhibited higher carbon content, which increased from 45.06 to 76.56%, and oxygen decreased from 45.28 to 11.86%. This occurred due to the thermal decomposition of lignocellulosic in raw materials during the carbonized process [39]. The RS1:3-800 showed the highest carbon content at 80.17% compared with RS and RS-Char due to increased temperature during the pyrolysis process [27].

Table 1
Proximate analysis and ultimate analysis of RS samples

Samples	Proximate contents (%wt)				Elemental contents (%wt)				
	Volatile	Fixed carbon	Moisture	Ash	C	H	O	N	S
RS	74.05	15.76	7.71	2.48	45.06	6.05	45.28	0.15	0.07
RS-Char	31.84	60.09	4.04	4.03	76.56	3.57	11.86	0.35	0.05
RS1:3-800	12.53	80.37	3.28	3.82	80.17	1.39	13.63	0.22	0.02

3.2 BET Analysis

The adsorption-desorption isotherms and pore size distribution (PSD) of RS samples are shown in Figure 2 and Figure 3. It was quite tough for the RS-Char sample to perform an adsorption demonstration because of its poor pore structure. According to The International Union of Pure and Applied Chemistry (IUPAC) classification, it can be found from Figure 2. that the absorption-

desorption isotherm curves of RS1:1-800, RS1:3-700, and RS1:3-800 samples showed type-I isotherm. The sharp increase of absorption at the relative pressure of $P/P_0 < 0.3$ indicates that samples have numerous amounts of micropores [40]. When micropores are filled, the adsorption increases slightly on the external surface. This behavior also indicates the existence of mesopore and macropore. Moreover, in case of the RS1:3-900 sample presented a combined property of type-I/IV isotherm. The sharp increase during absorption at the relative pressure around $P/P_0 < 0.3$ also like RS1:1-800, RS1:3-700, and RS1:3-800 samples, which refer to type I isotherm behavior. The appearance of the hysteresis loop at medium and the high pressure of $P/P_0 > 0.4$ (Type-IV) represents that the RS1:3-900 sample comprises a high ratio of mesopores [41,42].

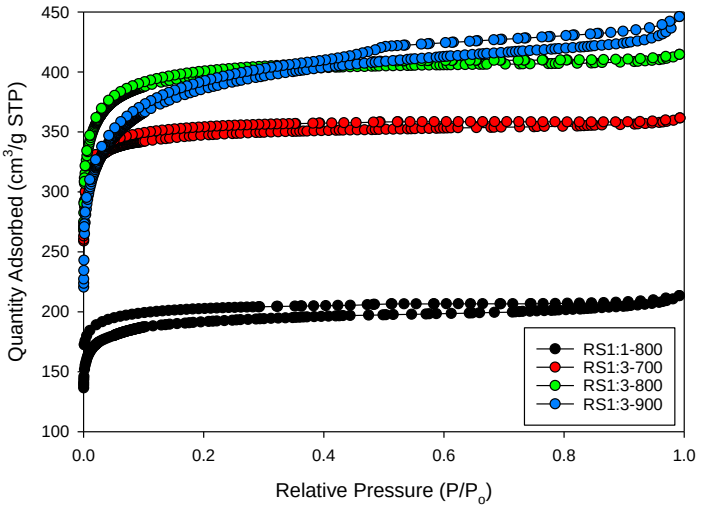

Fig. 2. The adsorption-desorption isotherms of RS samples

Figure 3 showed the pore size distribution curves (PSD) of RS1:1-800, RS1:3-700, RS1:3-800, and RS1:3-900, which further suggested that RS1:3-900 had apparent peaks in the micropore range of 1.16–2 nm and mesopore range of 2–5.92 nm. While RS1:1-800, RS1:3-700, and RS1:3-800 presented the major peaks at the micropore range (< 2 nm).

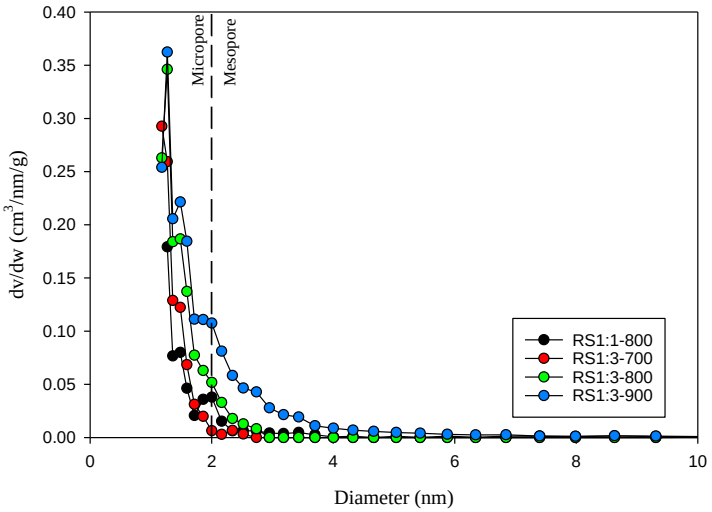

Fig. 3. Pore size distribution of RS samples

The BET surface area, total pore volume, micropore volume, mesopore volume, and average pore diameter were evaluated by BET Analysis and are shown in Table 2.

Table 2
Comparison of textural properties of RS samples

Samples	S_{BET} (m^2/g)	V_t (cm^3/g)	V_{mic} (cm^3/g)	V_{mes} (cm^3/g)	V_{mes}/V_t (%)	D_P (nm)
RS-Char	0.48	-	-	-	-	180.55
RS1:1-800	750.89	0.3289	0.1920	0.1369	41.63	1.75
RS1:3-700	1,417.77	0.5598	0.4546	0.1052	18.79	1.58
RS1:3-800	1,464.13	0.6405	0.3533	0.2873	44.85	1.63
RS1:3-900	1,574.39	0.6906	0.3241	0.3664	53.06	1.89

The RS-Char sample has a low surface area of around 0.48 m^2/g and a large average pore diameter of around 180.55 nm. After the activation process, the activated carbon had significantly increased surface area. The resulted of surface area of RS1:1-800, RS1:3-700, RS1:3-800, and RS1:3-900 samples were revealed as 750.89, 1,417.77, 1,464.13, and 1,574.39 m^2/g, respectively. The total pore volume of RS1:1-800, RS1:3-700, RS1:3-800, and RS1:3-900 samples were exhibited as 0.3289, 0.5598, 0.6405, and 0.6906 cm^3/g, respectively [27]. The RS1:3-900 samples had the highest V_{mes}/V_t at 53.06% and an average pore diameter of 1.89 nm, implying the RS1:3-900 huge mesopore amount of the activated carbon samples. In addition, the RS-activated carbon samples with the impregnation ratio of 1:3 have more surface area and total pore volume than the impregnation ratio of 1:1 [21,43]. Moreover, the increasing activation temperature can provide more surface area and more contain mesopore. Thus, for RS1:3-900, an observed increase of mesopores affords proper channels for ion transfer and penetration of electrolytes [20,43].

3.3 FESEM and EDX Analysis

The Field Emission Scanning Electron Microscope (FESEM) analysis was used to acquire information about the morphology of RS samples [14]. Figure 4(a) shows that the image of RS-Char carbonized at 400 °C reveals a hole with honeycomb structures. This is attributed to the metabolic channels and pore channels of rubber trees formed by the retreat of moisture and molecule gases produced by the thermal decomposition during the carbonization process [41]. The samples of RS1:1-800, RS1:3-700, RS1:3-800, and RS1:3-900 are presented in Figure 4(b) to Figure 4(e). The morphology images of RS1:3-700, RS1:3-800, and RS1:3-900 clearly show expanded microstructure and porosity, while the image of RS1:1-800 does not show a developed porosity on a flat surface. Therefore, with the increase of the KOH impregnation ratio, the surface of porous carbon becomes a well-formed porous structure [27]. In the case of the impregnation ratio of 1:3, the lower activation temperatures had produced a small pore. When the activation temperatures were increased, both the formation of micropores and mesopores. The formation of pores is due to increased surface area and the total pore volume in the activated carbon. The porous structure is highly important to be used as an efficient supercapacitor [44].

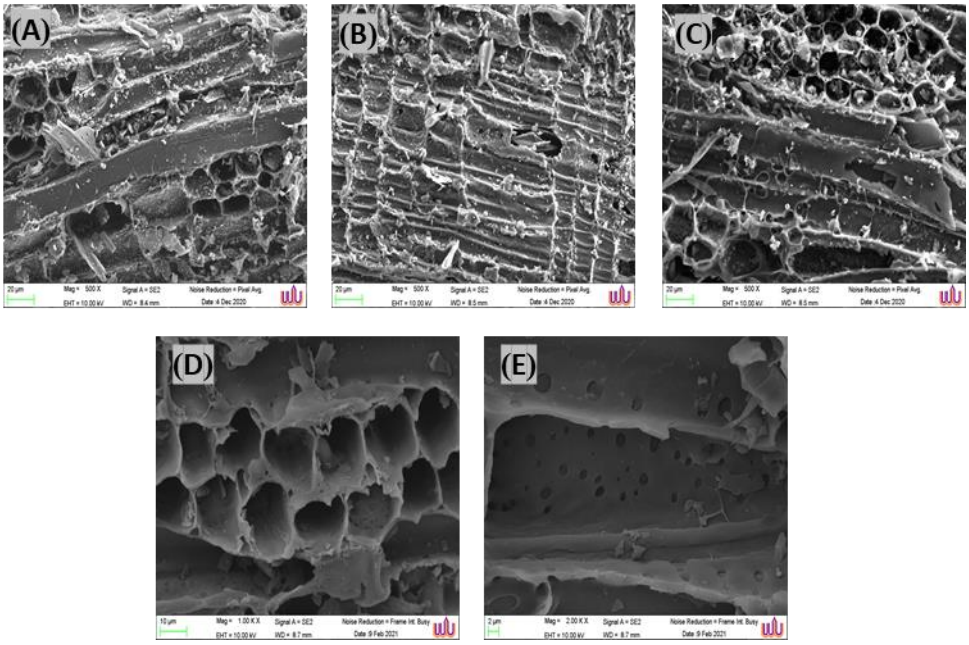

Fig. 4. FESEM Morphology images of (a)-(e) RS-Char, RS1:1-800, RS1:3-700, RS1:3-800, and RS1:3-900

Figure 5(a) to 5(e) presented the EDX peak of RS-Char, RS1:1-800, RS1:3-700, RS1:3-800, and RS1:3-900 samples, which insisted on the presence of high carbon and oxygen [20,21]. The elemental component such as phosphorus (P), Sulfur (S), and Silicon (Si) was found in the RS-Char and RS1:1-800 at low temperatures between 400-700 °C. However, these elements were eliminated when the temperature increased. For RS1:3-700, RS1:3-800, and RS1:3-900 samples, since biomass materials were used as raw materials, weak traces of other elements such as Calcium (Ca), Potassium (K), Magnesium (Mg) were detected [20].

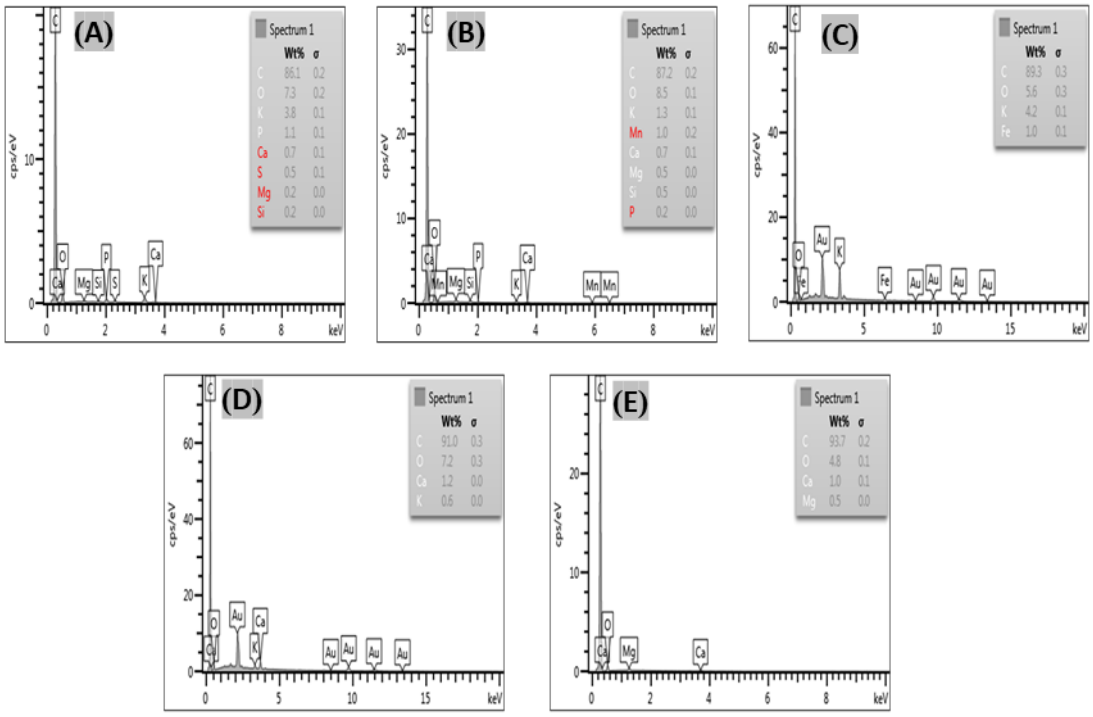

Fig. 5. EDX spectrum of (a)-(e) RS-Char, RS1:1-800, RS1:3-700, RS1:3-800, and RS1:3-900

3.4 FT-IR Spectral Analysis

The FT-IR analysis of rubberwood sawdust samples provides observational information on its property functional group. Figure 6 shows the FT-IR spectra of the RS-Char, RS1:3-700, RS1:3-800, and RS1:3-900 samples. It is found that the RS samples have different functional groups on the surface. The vibration at 3,419 cm^{-1}, 3382 cm^{-1} on the RS-1:3-800 and 3379 cm^{-1}, 3258 cm^{-1} on the RS-1:3-900 curve are mentioned to the O-H stretching band of the hydroxyl functional group with alcohol compound class [35]. For RS-Char, RS1:3-700, RS1:3-800, and RS1:3-900 spectrum, there are also two peaks at around 2,918-2,913 cm^{-1} and 2,842-2,851 cm^{-1}, which are consistent with the asymmetric and symmetric C-H stretching vibrations with alkene compound class in the as-prepared activated carbon samples [20].

In the case of the RS-Char, the frequency detected at 1579 cm^{-1} is related to the C=C stretching of the cyclic alkene functional group [45]. The weak peaks remarked at 874, 813, 755, and 715 cm^{-1} refer to the C-H bending vibrations in benzene derivatives. However, this existing functional group will disappear after activation at high temperatures. The sharp peak at around 1,430-1,433 cm^{-1}, which is attributed to O-H bending in the RS samples, was significantly decreased after the activation process. These results prove that the RS1:3-900 sample presents the carbon and oxygen-containing functional groups, which can transfer pronounced capacitance and conductivity to the activated carbon [21].

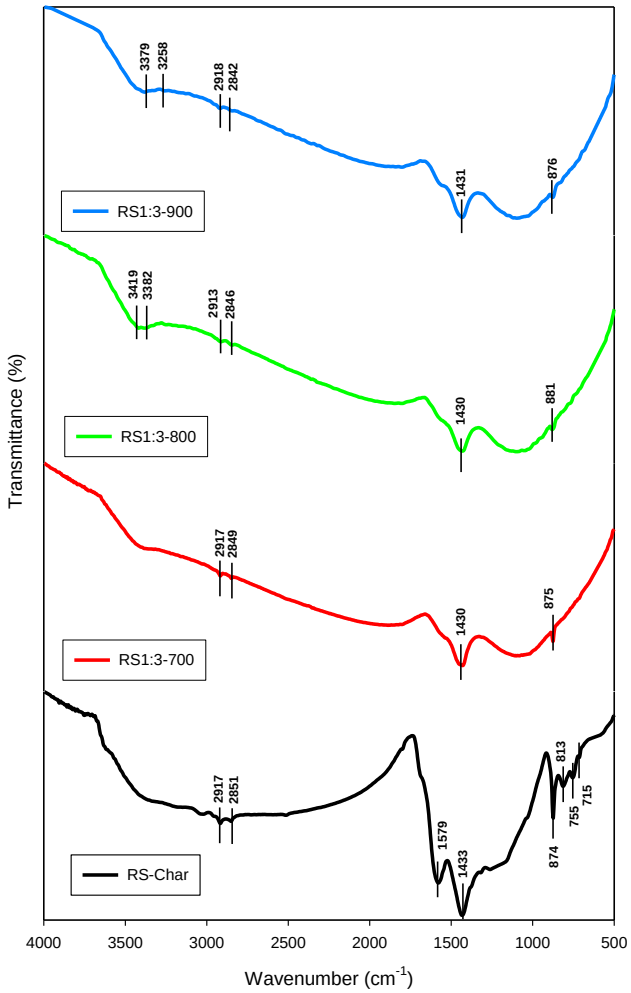

Fig. 6. The overlay FTIR spectra of the RS-Char, RS1:3-700, RS1:3-800, and RS1:3-900 samples

3.5 XRD Analysis

The X-ray diffraction pattern of the RS-Char, RS1:3-700, RS1:3-800 and RS1:3-900 samples are shown in Figure 7. The appearance of a broad peak by a weak peak indicates the amorphous nature of RS samples [20]. The noticeable peak of the RS-Char, RS1:3-700, RS1:3-800 and RS1:3-900 samples is situated at 2θ = 29.38°, composed of calcium carbonate ($CaCO_3$). When the activation temperature increases, the peak will be decreased. The calcium carbonate peaks correspond to JCPDS card number 01-072-1937 and suggest the rhombohedral crystal structure [46].

The XRD pattern of RS-Char at the carbonization temperature of 400 °C and RS1:3-700 also present two broad peaks at around 23° and 43° corresponding to (002) and (100) Bragg reflection planes, which refers to disordered carbon structure [41,47]. In comparison, the RS1:3-800 and RS1:3-900 hardly show (002) peaks and slightly (100) peaks. That means the carbon layers of activated carbon derived from the activation process have a lower graphitization degree than RS-char [41,48].

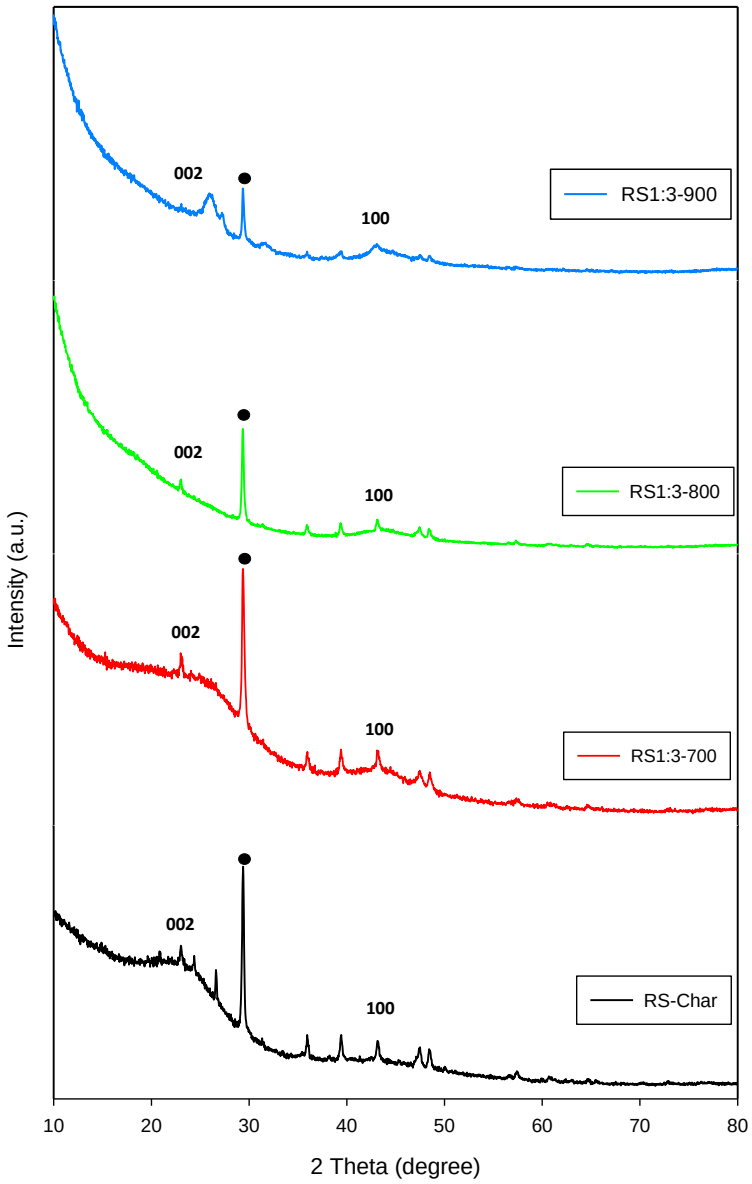

Fig. 7. XRD pattern of the RS-Char, RS1:3-700, RS1:3-800, and RS1:3-900 samples

3.6 Raman Spectral Analysis

Raman spectral of the RS-Char, RS1:3-700, RS1:3-800 and RS1:3-900 samples are shown in Figure 8. The graph of RS-Char presents two prominent peaks at 1359.2 cm^{-1} and 1586.7 cm^{-1}. In case of the RS1:3-700, RS1:3-800, and RS1:3-900 samples, there are also two peaks at 1338.7 cm^{-1} and 1587.3 cm^{-1}, 1341.0 cm^{-1} and 1585.1 cm^{-1}, 1339.9 cm^{-1} and 1576 cm^{-1}, respectively, which conform to the D band (defects and disorder structure) and the G band (graphitized carbons), respectively.

The intensity ratio (I_D/I_G) of RS-Char, RS1:3-700, RS1:3-800, and RS1:3-900 samples are 0.857, 0.843, 0.846, and 0.850, respectively. It implies that the lower intensity of RS1:3-700, RS1:3-800, and RS1:3-900 have a slightly higher graphitization yield and higher conductivity than RS-Char [20]. No apparent differences were revealed in the intensity ratio between RS-Char, RS1:3-700, RS1:3-800, and RS1:3-900 samples, which means KOH agents only develop the pore in the carbon materials without generating more additional disordered structure.

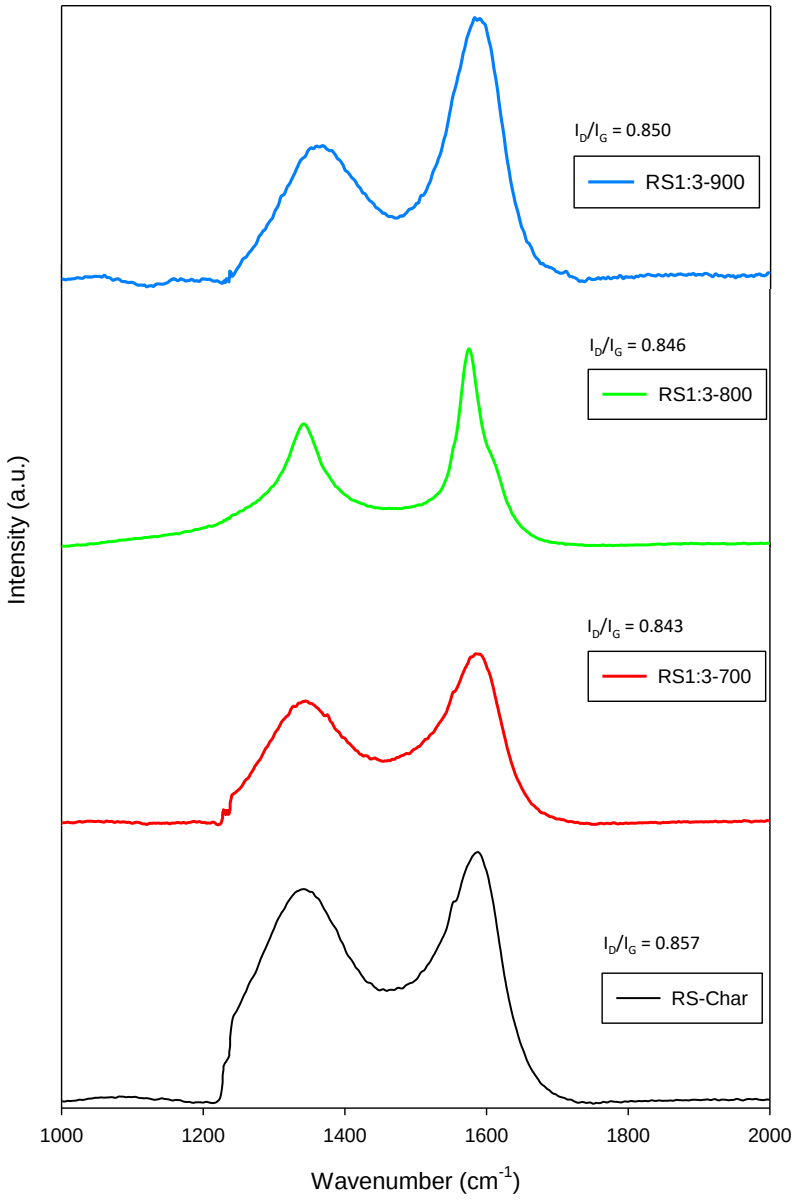

Fig. 8. Raman spectra of the RS-Char, RS1:3-700, RS1:3-800, and RS1:3-900 samples

3.7 Cyclic Voltammetry and Specific Capacitance Characteristic

The CV curves of the RS1:1-800, RS1:3-700, RS1:3-800, and RS1:3-900 samples are shown in Figure 9(a) to 9(d) to evaluate the electrochemical capacitance characteristic of the RS activated carbon with a different impregnation ratio and a different activation temperature. The CV test was carried out in 1 molar of aqueous KOH with the potential window of 0-1 V. The CV curves for RS1:1-800, RS1:3-700, RS1:3-800, and RS1:3-900 were determined at six different scan rates as 5, 10, 20, 50, 75, and 100 mV/s. The CV curves of RS1:1-800, RS1:3-700, RS1:3-800, and RS1:3-900 represent almost ideal EDLC behaviors, and the quasi-rectangular shape observed for all scan rates attributes to electrochemical capacitance [49].

Furthermore, the specific capacitance values were estimated as 23.16, 27.04, 37.30, and 54.08 F/g for the RS1:1-800, RS1:3-700, RS1:3-800, and RS1:3-900 electrode material, respectively, at the scan rate of 5 mV/s. The specific capacitance on various scan rates is shown in Figure 10, which gently decreases with increasing scan rate [20,43,50,51]. Thus, the specific capacitance of RS1:3-900 presented a higher value than the other RS samples (RS1:1-800, RS1:3-700, RS1:3-800) because of their higher surface area, which encouraged the accessibility of electrolyte ions at a high scan rate [21]. Moreover, for the RS1:3-900 sample, there is a reduction in microporous content while mesopores are increased, with rising activation temperature [21,52].

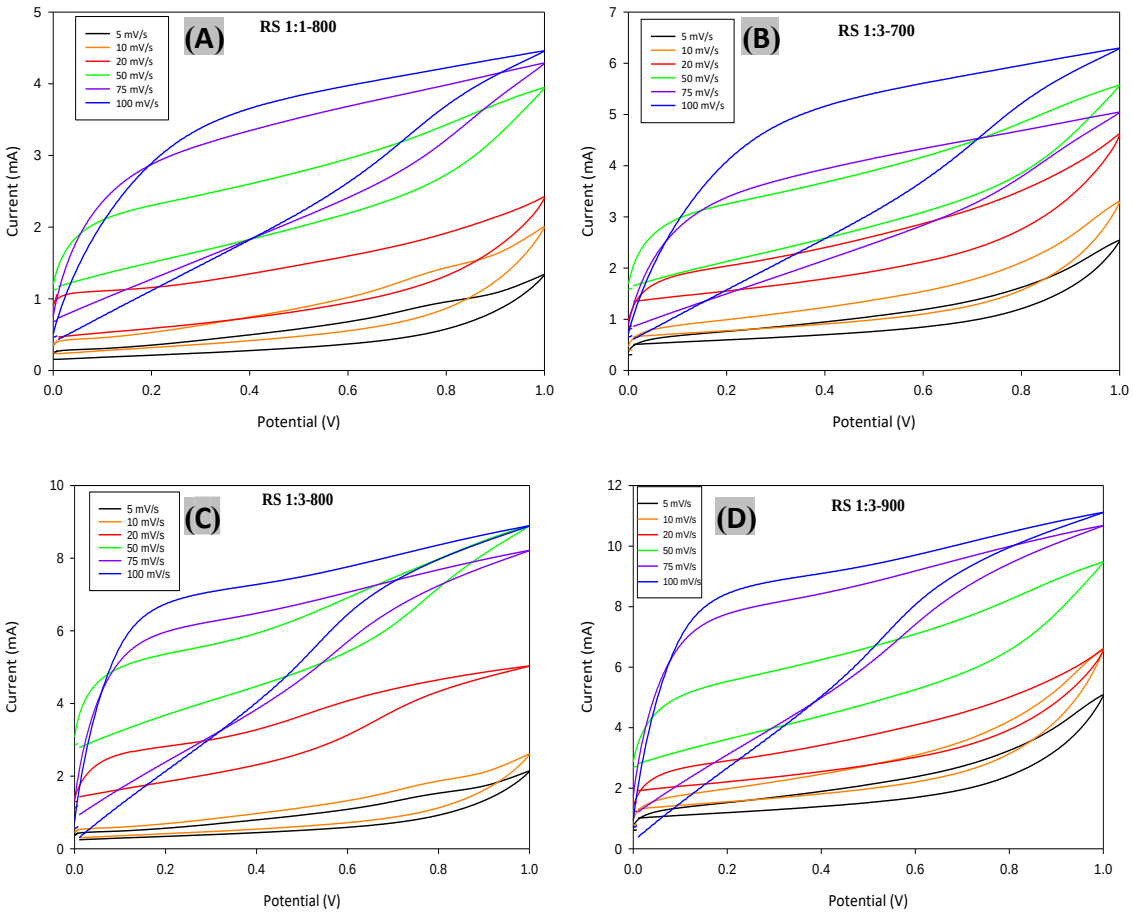

Fig. 9. CV curves of (a)-(d) RS-Char, RS1:3-700, RS1:3-800, and RS1:3-900 samples

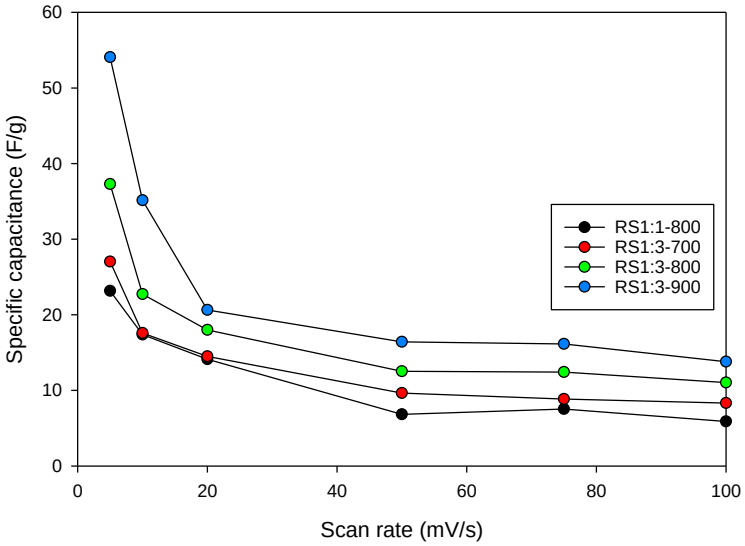

Fig. 10. Specific capacitance on the various scan rate

4. Conclusions

In this work, the rubberwood sawdust-derived activated carbon materials were prepared as electrode materials for the supercapacitors. The chemical activation process using KOH as an activation agent on the RS sample has improved the textural and electrochemical properties when increasing the impregnation ratio. The optimal impregnation ratio for the chemical activation of the RS sample was RS1:3-900, achieving the surface area and total pore volume of 1,574.39 m^2/g and 0.6906 cm^3/g, respectively. The well-developed micro-mesopores are suitable electrode materials for supercapacitor devices due to their abundance, low cost, eco-friendliness, and biomass residues. The specific capacitance characteristic of the RS1:3-900 samples exhibited the highest value of 54.08 F/g at a scan rate of 5 mV/s. Thus, it can be concluded that the activated carbon synthesized from rubberwood sawdust through chemical activation with KOH has the potential to use as an effective electrode for supercapacitor.

Acknowledgment

The authors are appreciative of PSU Energy System Research Institute for research funds, Prince of Songkla University for funding (Grant no. the ENG6201078S year 2019), Southern Biomass Fuel Co., Ltd. for the rubberwood sawdust, and, Metallurgy and Materials Science Research Institute, Chulalongkorn University for instruction and providing equipment.

References

[1] Radenahmad, Nikdalila, Atia Tasfiah Azad, Muhammad Saghir, Juntakan Taweekun, Muhammad Saifullah Abu Bakar, Md Sumon Reza, and Abul Kalam Azad. "A review on biomass derived syngas for SOFC based combined heat and power application." *Renewable and Sustainable Energy Reviews* 119 (2020): 109560. https://doi.org/10.1016/j.rser.2019.109560

[2] Reza, Md Sumon, Nurnazurah Binti Haji Ahmad, Shammya Afroze, Juntakan Taweekun, Mohsen Sharifpur, and Abul Kalam Azad. "Hydrogen Production from Water Splitting Through Photocatalytic Activity of Carbon-Based Materials, A Review." *Chemical Engineering & Technology* (2022). https://doi.org/10.1002/ceat.202100513

[3] Afif, Ahmed, Sheikh MH Rahman, Atia Tasfiah Azad, Juliana Zaini, Md Aminul Islan, and Abul Kalam Azad. "Advanced materials and technologies for hybrid supercapacitors for energy storage-a review." *Journal of Energy Storage* 25 (2019): 100852. https://doi.org/10.1016/j.est.2019.100852

[4] Zhang, Tao, Jilun Liu, Cheng Wang, Xuanye Leng, Yao Xiao, and Lei Fu. "Synthesis of graphene and related two-dimensional materials for bioelectronics devices." *Biosensors and Bioelectronics* 89 (2017): 28-42. https://doi.org/10.1016/j.bios.2016.06.072

[5] Miller, John R. "Perspective on electrochemical capacitor energy storage." *Applied Surface Science* 460 (2018): 3-7. https://doi.org/10.1016/j.apsusc.2017.10.018

[6] Fernando, Jayathu. "Electrical double-layer capacitors." In *Energy Storage Devices for Renewable Energy-Based Systems*, pp. 199-237. Academic Press, 2021. https://doi.org/10.1016/B978-0-12-820778-9.00004-8

[7] Mathis, Tyler S., Narendra Kurra, Xuehang Wang, David Pinto, Patrice Simon, and Yury Gogotsi. "Energy storage data reporting in perspective-guidelines for interpreting the performance of electrochemical energy storage systems." *Advanced Energy Materials* 9, no. 39 (2019): 1902007. https://doi.org/10.1002/aenm.201902007

[8] Saikia, Binoy K., Santhi Maria Benoy, Mousumi Bora, Joyshil Tamuly, Mayank Pandey, and Dhurbajyoti Bhattacharya. "A brief review on supercapacitor energy storage devices and utilization of natural carbon resources as their electrode materials." *Fuel* 282 (2020): 118796. https://doi.org/10.1016/j.fuel.2020.118796

[9] Alqurneh, Ahmad, Aida Mustapha, and Nurfadhlina Mohd Sharef. "A Partitioning-based Approach for Clustering COVID-19 Drugs and Co-Medication for Safe Use." *International Journal of Integrated Engineering* 12, no. 5 (2020): 224-232. https://doi.org/10.30880/ijie.2020.12.05.029

[10] Reza, Md Sumon, Cheong Sing Yun, Shammya Afroze, Nikdalila Radenahmad, Muhammad S. Abu Bakar, Rahman Saidur, Juntakan Taweekun, and Abul K. Azad. "Preparation of activated carbon from biomass and its' applications in water and gas purification, a review." *Arab Journal of Basic and Applied Sciences* 27, no. 1 (2020): 208-238. https://doi.org/10.1080/25765299.2020.1766799

[11] Farma, Rakhmawati, Mohamad Deraman, A. Awitdrus, I. A. Talib, E. Taer, N. H. Basri, J. G. Manjunatha, M. M. Ishak, B. N. M. Dollah, and S. A. Hashmi. "Preparation of highly porous binderless activated carbon electrodes from fibres of oil palm empty fruit bunches for application in supercapacitors." *Bioresource Technology* 132 (2013): 254-261. https://doi.org/10.1016/j.biortech.2013.01.044

[12] Ismanto, Andrian Evan, Steven Wang, Felycia Edi Soetaredjo, and Suryadi Ismadji. "Preparation of capacitor's electrode from cassava peel waste." *Bioresource Technology* 101, no. 10 (2010): 3534-3540. https://doi.org/10.1016/j.biortech.2009.12.123

[13] Gómez-Serrano, Vd, E. M. Cuerda-Correa, M. C. Fernandez-Gonzalez, M. F. Alexandre-Franco, and A. Macias-Garcia. "Preparation of activated carbons from chestnut wood by phosphoric acid-chemical activation. Study of microporosity and fractal dimension." *Materials Letters* 59, no. 7 (2005): 846-853. https://doi.org/10.1016/j.matlet.2004.10.064

[14] Chen, Mingde, Xueya Kang, Tuerdi Wumaier, Junqing Dou, Bo Gao, Ying Han, Guoqing Xu, Zhiqiang Liu, and Lu Zhang. "Preparation of activated carbon from cotton stalk and its application in supercapacitor." *Journal of Solid State Electrochemistry* 17, no. 4 (2013): 1005-1012. https://doi.org/10.1007/s10008-012-1946-6

[15] Rufford, Thomas E., Denisa Hulicova-Jurcakova, Zhonghua Zhu, and Gao Qing Lu. "Nanoporous carbon electrode from waste coffee beans for high performance supercapacitors." *Electrochemistry Communications* 10, no. 10 (2008): 1594-1597. https://doi.org/10.1016/j.elecom.2008.08.022

[16] Peng, Chao, Xing-bin Yan, Ru-tao Wang, Jun-wei Lang, Yu-jing Ou, and Qun-ji Xue. "Promising activated carbons derived from waste tea-leaves and their application in high performance supercapacitors electrodes." *Electrochimica Acta* 87 (2013): 401-408. https://doi.org/10.1016/j.electacta.2012.09.082

[17] Li, Xiao, Wei Xing, Shuping Zhuo, Jin Zhou, Feng Li, Shi-Zhang Qiao, and Gao-Qing Lu. "Preparation of capacitor's electrode from sunflower seed shell." *Bioresource Technology* 102, no. 2 (2011): 1118-1123. https://doi.org/10.1016/j.biortech.2010.08.110

[18] Elmouwahidi, Abdelhakim, Zulamita Zapata-Benabithe, Francisco Carrasco-Marín, and Carlos Moreno-Castilla. "Activated carbons from KOH-activation of argan (Argania spinosa) seed shells as supercapacitor electrodes." *Bioresource Technology* 111 (2012): 185-190. https://doi.org/10.1016/j.biortech.2012.02.010

[19] Lv, Yaokang, Lihua Gan, Mingxian Liu, Wei Xiong, Zijie Xu, Dazhang Zhu, and Dominic S. Wright. "A self-template synthesis of hierarchical porous carbon foams based on banana peel for supercapacitor electrodes." *Journal of Power Sources* 209 (2012): 152-157. https://doi.org/10.1016/j.jpowsour.2012.02.089

[20] Elaiyappillai, Elanthamilan, Rajkumar Srinivasan, Yesuraj Johnbosco, Premkumar Devakumar, Kumaresan Murugesan, Karthikeyan Kesavan, and Princy Merlin Johnson. "Low cost activated carbon derived from Cucumis melo fruit peel for electrochemical supercapacitor application." *Applied Surface Science* 486 (2019): 527-538. https://doi.org/10.1016/j.apsusc.2019.05.004

[21] Srinivasan, Rajkumar, Elanthamilan Elaiyappillai, Hepsiba Paul Pandian, Renganathan Vengudusamy, Princy Merlin Johnson, Shen-Ming Chen, and Ramasamy Karvembu. "Sustainable porous activated carbon from Polyalthia longifolia seeds as electrode material for supercapacitor application." *Journal of Electroanalytical Chemistry* 849 (2019): 113382. https://doi.org/10.1016/j.jelechem.2019.113382

[22] Mi, Juan, Xiao-Rong Wang, Rui-Jun Fan, Wen-Hui Qu, and Wen-Cui Li. "Coconut-shell-based porous carbons with a tunable micro/mesopore ratio for high-performance supercapacitors." *Energy & Fuels* 26, no. 8 (2012): 5321-5329. https://doi.org/10.1021/ef3009234

[23] Yang, Kunbin, Jinhui Peng, Chandrasekar Srinivasakannan, Libo Zhang, Hongying Xia, and Xinhui Duan. "Preparation of high surface area activated carbon from coconut shells using microwave heating." *Bioresource Technology* 101, no. 15 (2010): 6163-6169. https://doi.org/10.1016/j.biortech.2010.03.001

[24] Winata, I. Made Putra Arya, Putu Emilia Dewi, Putu Brahmanda Sudarsana, and Made Sucipta. "Air-Flow Simulation in Child Respirator for Covid-19 Personal Protection Equipment Using Bamboo-Based Activated Carbon Filter." *Journal of Advanced Research in Fluid Mechanics and Thermal Sciences* 91, no. 1 (2022): 83-91. https://doi.org/10.37934/arfmts.91.1.8391

[25] Mokti, Nawwarah, Azry Borhan, Siti Nur Azella Zaine, and Hayyiratul Fatimah Mohd Zaid. "Synthesis and Characterisation of Pyridinium-Based Ionic Liquid as Activating Agent in Rubber Seed Shell Activated Carbon Production for CO_2 Capture." *Journal of Advanced Research in Fluid Mechanics and Thermal Sciences* 82, no. 1 (2021): 85-95. https://doi.org/10.37934/arfmts.82.1.8595

[26] Johnson, Kenneth C. "A decarbonization strategy for the electricity sector: New-source subsidies." *Energy Policy* 38, no. 5 (2010): 2499-2507. https://doi.org/10.1016/j.enpol.2009.12.044

[27] Thongpat, Wasutha, Juntakan Taweekun, and Kittinan Maliwan. "Synthesis and characterization of microporous activated carbon from rubberwood by chemical activation with KOH." *Carbon Letters* 31, no. 5 (2021): 1079-1088. https://doi.org/10.1007/s42823-020-00224-z

[28] Ayinla, Ridwan Tobi, J. O. Dennis, H. M. Zaid, Y. K. Sanusi, Fahad Usman, and L. L. Adebayo. "A review of technical advances of recent palm bio-waste conversion to activated carbon for energy storage." *Journal of Cleaner Production* 229 (2019): 1427-1442. https://doi.org/10.1016/j.jclepro.2019.04.116

[29] Yang, Kun, Lianghong Zhu, Jingjing Yang, and Daohui Lin. "Adsorption and correlations of selected aromatic compounds on a KOH-activated carbon with large surface area." *Science of The Total Environment* 618 (2018): 1677-1684. https://doi.org/10.1016/j.scitotenv.2017.10.018

[30] Zaini, Muhammad Abbas Ahmad, and Mohd Johari Kamaruddin. "Critical issues in microwave-assisted activated carbon preparation." *Journal of Analytical and Applied Pyrolysis* 101 (2013): 238-241. https://doi.org/10.1016/j.jaap.2013.02.003

[31] Zequine, Camila, C. K. Ranaweera, Z. Wang, Sweta Singh, Prashant Tripathi, O. N. Srivastava, Bipin Kumar Gupta et al. "High Per formance and Flexible Supercapacitors based on Carbonized Bamboo Fibers for Wide Temperature Applications." *Scientific Reports* 6 (2016): 31704. https://doi.org/10.1038/srep31704

[32] Hsieh, Tzu-Hsien, Hao-Lun Wang, Guan-Tin Yu, Guang-Meng Huang, and Jarrn-Horng Lin. "Meso-pore dominant activated carbon from spent coffee grounds for high-performance electrochemical capacitors in organic electrolyte." *Journal of Environmental Chemical Engineering* 9, no. 6 (2021): 106418. https://doi.org/10.1016/j.jece.2021.106418

[33] Phainuphong, S., J. Taweekun, T. Theppaya, and K. Maliwan. "Synthesis and characterization of activated carbon derived from rubberwood sawdust by using KOH/KMnO4 as multiple function activation agents." In *IOP Conference Series: Materials Science and Engineering*, vol. 1163, no. 1, p. 012019. IOP Publishing, 2021. https://doi.org/10.1088/1757-899X/1163/1/012019

[34] Negara, Dewa Ngakan Ketut Putra, Tjokorda Gde Tirta Nindhia, I. Wayan Surata, Fadjar Hidajat, and Made Sucipta. "Textural characteristics of activated carbons derived from tabah bamboo manufactured by using H_3PO_4 chemical activation." *Materials Today: Proceedings* 22 (2020): 148-155. https://doi.org/10.1016/j.matpr.2019.08.030

[35] Reza, Md Sumon, Ashfaq Ahmed, Wahyu Caesarendra, Muhammad S. Abu Bakar, Shahriar Shams, R. Saidur, Navid Aslfattahi, and Abul K. Azad. "Acacia holosericea: an invasive species for bio-char, bio-oil, and biogas production." *Bioengineering (Basel)* 6, no. 2 (2019): 33. https://doi.org/10.3390/bioengineering6020033

[36] Reza, Md Sumon, Shammya Afroze, Muhammad SA Bakar, Rahman Saidur, Navid Aslfattahi, Juntakan Taweekun, and Abul K. Azad. "Biochar characterization of invasive Pennisetum purpureum grass: effect of pyrolysis temperature." *Biochar* 2, no. 2 (2020): 239-251. https://doi.org/10.1007/s42773-020-00048-0

[37] Açıkyıldız, Metin, Ahmet Gürses, and Semra Karaca. "Preparation and characterization of activated carbon from plant wastes with chemical activation." *Microporous and Mesoporous Materials* 198 (2014): 45-49. https://doi.org/10.1016/j.micromeso.2014.07.018

[38] Yorgun, Sait, and Derya Yıldız. "Preparation and characterization of activated carbons from Paulownia wood by chemical activation with H3PO4." *Journal of the Taiwan Institute of Chemical Engineers* 53 (2015): 122-131. https://doi.org/10.1016/j.jtice.2015.02.032

[39] Reza, M. S., S. Afroze, A. K. Azad, R. S. Sukri, S. Shams, J. Taweekun, M. Saghir, N. Phusunti, and M. S. Abu Bakar. "Thermochemical characterization of invasive Axonopus compressus grass as a renewable energy source." In *IOP*

Conference Series: Materials Science and Engineering, vol. 991, no. 1, p. 012074. IOP Publishing, 2020. https://doi.org/10.1088/1757-899X/991/1/012074

[40] Yurdakal, Sedat, Corrado Garlisi, Levent Özcan, Marianna Bellardita, and Giovanni Palmisano. "(Photo) catalyst characterization techniques: adsorption isotherms and BET, SEM, FTIR, UV-Vis, photoluminescence, and electrochemical characterizations." In *Heterogeneous Photocatalysis*, pp. 87-152. Elsevier, 2019. https://doi.org/10.1016/B978-0-444-64015-4.00004-3

[41] Cheng, Youliang, Linlin Wu, Changqing Fang, Tiehu Li, Jing Chen, Mannan Yang, and Qingling Zhang. "Synthesis of porous carbon materials derived from laminaria japonica via simple carbonization and activation for supercapacitors." *Journal of Materials Research and Technology* 9, no. 3 (2020): 3261-3271. https://doi.org/10.1016/j.jmrt.2020.01.022

[42] Feng, Haobin, Hang Hu, Hanwu Dong, Yong Xiao, Yijin Cai, Bingfu Lei, Yingliang Liu, and Mingtao Zheng. "Hierarchical structured carbon derived from bagasse wastes: a simple and efficient synthesis route and its improved electrochemical properties for high-performance supercapacitors." *Journal of Power Sources* 302 (2016): 164-173. https://doi.org/10.1016/j.jpowsour.2015.10.063

[43] Yang, Cheol-Soo, Yun Su Jang, and Hae Kyung Jeong. "Bamboo-based activated carbon for supercapacitor applications." *Current Applied Physics* 14, no. 12 (2014): 1616-1620. https://doi.org/10.1016/j.cap.2014.09.021

[44] Afroze, Shammya, AfizulHakem Karim, Quentin Cheok, Sten Eriksson, and Abul K. Azad. "Latest development of double perovskite electrode materials for solid oxide fuel cells: a review." *Frontiers in Energy* 13, no. 4 (2019): 770-797. https://doi.org/10.1007/s11708-019-0651-x

[45] Reza, Md Sumon, Shafi Noor Islam, Shammya Afroze, Muhammad S. Abu Bakar, Rahayu S. Sukri, Saidur Rahman, and Abul K. Azad. "Evaluation of the bioenergy potential of invasive Pennisetum purpureum through pyrolysis and thermogravimetric analysis." *Energy, Ecology and Environment* 5, no. 2 (2020): 118-133. https://doi.org/10.1007/s40974-019-00139-0

[46] Ali, Zulfiqar, Muhammad Tahir, Chuanbao Cao, Asif Mahmood, Nasir Mahmood, Faheem K. Butt, Muhammad Tanveer et al. "Solid waste for energy storage material as electrode of supercapacitors." *Materials Letters* 181 (2016): 191-195. https://doi.org/10.1016/j.matlet.2016.05.159

[47] Yan, Dong, Caiyan Yu, Xiaojie Zhang, Wei Qin, Ting Lu, Bingwen Hu, Huili Li, and Likun Pan. "Nitrogen-doped carbon microspheres derived from oatmeal as high capacity and superior long life anode material for sodium ion battery." *Electrochimica Acta* 191 (2016): 385-391. https://doi.org/10.1016/j.electacta.2016.01.105

[48] Su, Jian, Changqing Fang, Mannan Yang, Youliang Cheng, Zhen Wang, Zhigang Huang, and Caiyin You. "A controllable soft-templating approach to synthesize mesoporous carbon microspheres derived from d-xylose via hydrothermal method." *Journal of Materials Science & Technology* 38 (2020): 183-188. https://doi.org/10.1016/j.jmst.2019.03.050

[49] Adinaveen, T., L. John Kennedy, J. Judith Vijaya, and G. Sekaran. "Studies on structural, morphological, electrical and electrochemical properties of activated carbon prepared from sugarcane bagasse." *Journal of industrial and Engineering Chemistry* 19, no. 5 (2013): 1470-1476. https://doi.org/10.1016/j.jiec.2013.01.010

[50] Kim, Hee Soo, Muhammad Awais Abbas, Min Seok Kang, Hyuna Kyung, Jin Ho Bang, and Won Cheol Yoo. "Study of the structure-properties relations of carbon spheres affecting electrochemical performances of EDLCs." *Electrochimica Acta* 304 (2019): 210-220. https://doi.org/10.1016/j.electacta.2019.02.121

[51] Karnan, M., K. Subramani, P. K. Srividhya, and M. Sathish. "Electrochemical studies on corncob derived activated porous carbon for supercapacitors application in aqueous and non-aqueous electrolytes." *Electrochimica Acta* 228 (2017): 586-596. https://doi.org/10.1016/j.electacta.2017.01.095

[52] Deng, Wenfang, Yijia Zhang, Lu Yang, Yueming Tan, Ming Ma, and Qingji Xie. "Sulfur-doped porous carbon nanosheets as an advanced electrode material for supercapacitors." *RSC Advances* 5, no. 17 (2015): 13046-13051. https://doi.org/10.1039/C4RA14820G